2014

ISSN : 0974 - 7435 Volume 10 Issue 8

BioTechnology

An Indian Journal

FULL PAPER

BTAIJ, 10(8), 2014 [2923-2931]

# Numerical analysis and experimental study of magnetic flux leakage detection for the weld defect

**Cui Wei[1], Zhao Peng-xiao[2]**

**[1]College of Mechanical Science & Engineering, Northeast Petroleum University, Daqing Heilongjiang 163318, (CHINA)**

**[2]Ninth Oil Production Plant of Daqing Oilfield Co., Ltd, Daqing Heilongjiang 163853, (CHINA)**

**Email : cuiweivv@126.com**

## ABSTRACT

This paper presents a new approach based on the method of magnetic flux leakage (MFL) for the one-sided butt weld (OSBW) in order to detect and identify the weld defect. Combining the numerical analysis and experimental research method, a new non-contact scanning MFL system (NCSMFLS) for the weld defect is designed and implemented whose magnetization direction is perpendicular to marching direction. Then NCSMFLS is used continuously in the weld defect such as the rectangular slot in the weld and the rectangular slot in the weld heat-affected zone by the rectangular slot defect to simulate the crack defect, afterwards, this paper reviews the characteristics such as size and distribution of leakage magnetic field (LMF) of the above-mentioned two kinds of positions. Also, the fitting curve by least squares method and polynomial regression equation for two kinds of positions are obtained. The outcomes indicate that the numerical simulation results and experimental results match each other well and their correlation coefficient of the original data: rectangular slot in the weld $R_{wr}$=0.9764; rectangular slot in the weld heat-affected zone $R_{hr}$=0.943, furthermore, the results verify the feasibility and the validity for the suggested detection system.

## KEYWORDS

One-sided welding butt weld; Magnetic flux leakage testing; Numerical simulation; Experimental study; Rectangular slot defect.

© Trade Science Inc.

## INTRODUCTION

Welding is modern industrial base, and welding equipments easily fail in the course of fabricating and service. Then the existence of the welding defect will affect the quality of the welded joints and the safety use of the structural parts, and the crack is a major defect what affects the weld mechanical properties. For the welded structures are more sensitive to the cracks, when there are cracks in the weld, the mechanical properties will be greatly affected. If the local cracks of the welded structures extend to the whole and then make the formation of the penetrating defects which may reduce the carrying capacity of the equipments and even lead to accidents[1,2]. Consequently, it is necessary to test the weld by using advanced Non-Destructive Testing (NDT). Also, it can prevent accidents what has important social and economic benefits. At present, it is usually using Radiographic Testing (RT) and Ultrasonic Testing (UT) et al. for on-line inspection of the weld at home and abroad[3-7]. Furthermore, magnetic flux leakage (MFL) technology plays an important role for testing the crack and the corrosion in the tank bottom and the pipeline. However, MFL is seldom applied on testing for the weld defects at home and abroad.

Based on the principle of the weld MFL testing, this paper takes the rectangular slot in the weld and the rectangular slot in the weld heat-affected zone (WHAZ) as the research object by the rectangular slot defect to simulate the crack defect. Then a new non-contact scanning MFL system (NCSMFLS) for the weld defect is designed and implemented. Also, leakage magnetic field (LMF) of rectangular slot defect of two different positions is simulation analyzed. Afterwards, numerical calculation contrast curves of three-dimensional LMF are presented, and the characteristics such as size and distribution of LMF of the above-mentioned two kinds of positions are summarized. Then the fitting curve, polynomial regression equation and correlation coefficient R for two kinds of positions are obtained respectively. Furthermore, it is to explore a new way that this paper uses the new magnetic structure for the crack detection in the weld with different locations, and this method provides a reference for weld MFL in the engineering.

## PRINCIPLE

The principle of MFL testing of the butt weld has been introduced in the reference[7]. And in MFL system for the weld, the magnetic induction (MI) $B$ which is collected by the sensor consists of three parts:

$$B=B_1+B_2+B_3 \quad (1)$$

Formula (1):
$B_1$- air-coupled magnetic field (T);
$B_2$- LMF generated by the weld (T);
$B_3$- LMF generated by the defect (T).

Whether there is a weld or a defect in the base metal, air-coupled magnetic field exists and $B_1$ is a constant. When there is a weld, LMF is measured by stacking air-coupled magnetic field $B_1$ and LMF $B_2$ generated by the weld. Afterwards, when there is defect in the weld surface or in the weld, LMF is measured by stacking air-coupled magnetic field $B_1$, LMF $B_2$ generated by the weld and LMF $B_3$ generated by the defect.

## NUMERICAL SIMULATION

It is one of the major defects that the crack affects the weld strength. Also, the cracks are broadly divided into hot crack and cold crack, and they can be distributed in the weld and WHAZ. Moreover, the hot crack is usually cracking along the longitudinal direction of the weld center, and the cold crack is generally distributed in WHAZ. Then the rectangular slot with a certain width, a certain depth and a certain length are simulated the crack in the numerical analysis. Furthermore, take the plate thickness 8mm, the weld width 18mm and the weld reinforcement 3mm as the example, and it is established respectively in the weld and WHAZ that the rectangular slot is length 40mm, width 1mm, and the depth

which reaches 60% of the plate thickness. Figure 1 shows the diagrams of two finite element method (FEM) models. Also, this paper selects sparse director solve, and convergence condition is FEM software default setting: L2 norm $\left\|\{R\}\right\|_2 = \left(\sum R_i^2\right)^{\frac{1}{2}}$.

To get LMF distribution characteristics when the rectangular slot in different locations of the weld, the same time as the service life of the weld and the steel plate are directly related to the depth of the defect. Thus study LMF characteristics changes of the rectangular slot defect from the geometry size changes of the single depth direction (The other direction dimensions are to remain unchanged.).

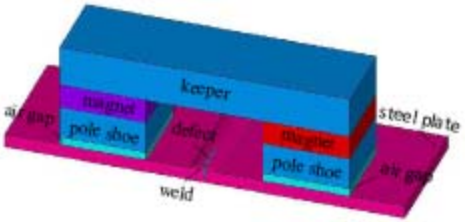


**(a) rectangular slot in the weld**

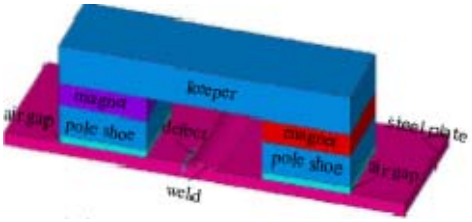


**(b) rectangular slot in WHAZ**

**Figure 1 : 3D FEM model**

FEM model of rectangular slot defects of different depths in one-sided weld and WHAZ are established respectively to simulate the crack. Then the plate thickness is 8mm, the weld reinforcement is 3mm, and the weld width 18mm. The rectangular slot sizes of two positions are length 40mm, width 1mm.

Also, the rectangular slot depths in the weld reach 20%, 40%, 60%, and 80% of the plate thickness respectively (Add weld reinforcement 3mm to percentage of the plate thickness.), that 4.6mm, 6.2mm, 7.8mm, 9.4mm; the rectangular slot depth in WHAZ are from 20%, 40%, 60%, and 80% of the plate thickness respectively, that 1.6mm, 3.2mm, 4.8mm, 6.4mm. Also, for the comparative analysis, establish the models of the steel plate without weld and the weld without defect. Afterwards, the MI components are extracted from the corresponding path. Furthermore, Figure 2 and Figure 3 show the contrast curves of MI component of LMF under three kinds: defects of different depths under the different positions of two kinds, the steel plate without weld and the weld without defect.

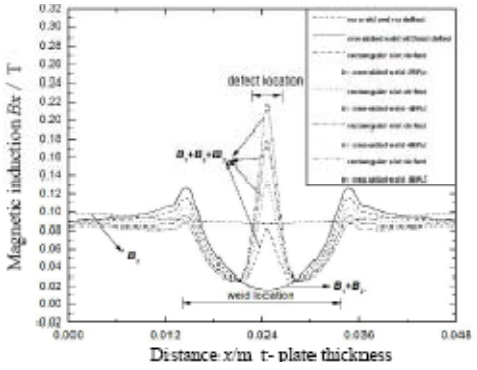


**(a) horizontal component**

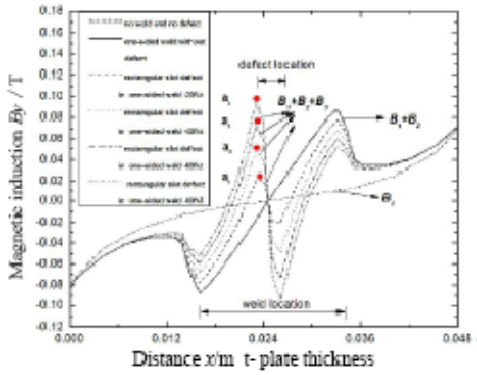


**(b) vertical component**

**Figure 2 : Contrast curves of magnetic induction component of the rectangular slot of different depths in the weld**

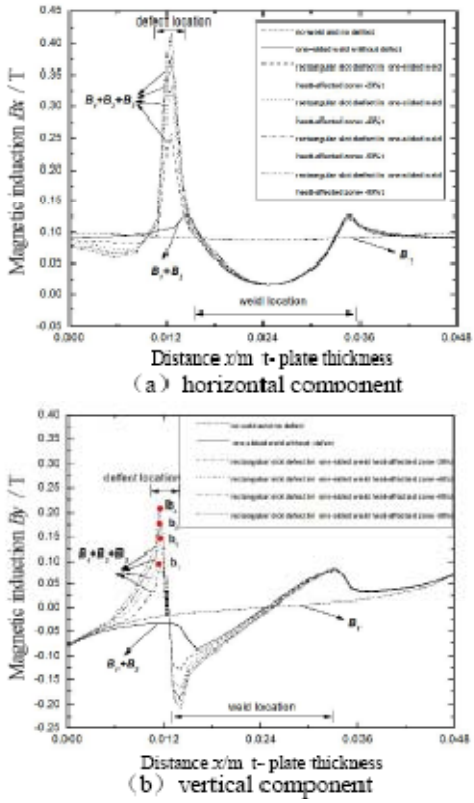


**Figure 3 : Contrast curves of magneticinduction component of the rectangular slot of different depths in WHAZ**

In Figure 2 or Figure 3, air-coupled magnetic field $B_1$ is collected by the sensor when the steel plate has no weld. Comparing to the non-weld, there is a trough of the horizontal component *Bx* curve for the one-sided weld LMF; first there is a trough and after there is a peak of the vertical component *By* curve for one-sided weld LMF. This is because the weld is ferromagnetic, part of the magnetic lines of force traverse through the weld and make the plate magnetic flux density reduce. By stacking air-coupled magnetic field $B_1$ and LMF $B_2$ generated by the weld, the curves have been shown in Figure 2 and Figure 3.

From Figure 2, compare to the non-defect, the MI horizontal component *Bx* curve of the rectangular slot in the weld shows a trough into a peak; first there is a peak and after there is a trough of the vertical component *By* curve. In addition, under certain scanning direction, which is the peak and the trough of vertical component curve of the weld itself shows in reverse order. Because the rectangular

slot in the plate is thinning out, then magnetic flux density of the steel plate is increased, also, the LMF density is increased. The results are due to LMF $B_3$ generated by the defect through superimposing on air-coupled magnetic field $B_1$ and LMF $B_2$ generated by the weld. In addition, from Figure 2, the peaks of MI components of LMF are increasing with the rectangular slot depth increasing.

From Figure 3, when the rectangular slot in WHAZ, because the position of the rectangular slot deviates from the centerline of the entire magnetic structure, the curves of the MI components all show the asymmetry characteristics under the different depths cracks. Also, both from Figure 3a and Figure 3b, compare to the non-defect, the curves of the MI components for the rectangular slot in WHAZ all have more than a peak at the defect location. The results are due to LMF $B_3$ generated by the defect through superimposing on air-coupled magnetic field $B_1$ and LMF $B_2$ generated by the weld. In addition, from Figure 3, the peaks of MI components of LMF are increasing with the rectangular slot depth increasing.

## EXPERIMENTAL STUDY

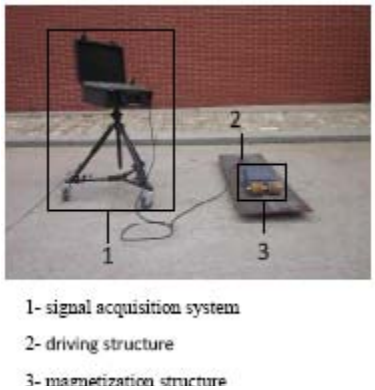


**Figure 4 : NCSMFLS for the weld**

The marching direction of MFL instrument and magnetization direction were in the same direction in the past. This paper aims at the detection characteristics of the weld structure, thus the magnetization direction is rotated 90 degree. Namely the instrument advances forward along the weld and the magnetization direction is perpendicular to weld line. The NCSMFLS for the weld is shown in Figure 4.

The rectangular slot defects in the weld and the rectangular slot defects in WHAZ are prefabricated in the experiment board of one-sided butt weld which is reinforcement 3mm and width 18mm. Figure 5 shows the diagram of the weld experiment board, geometry size of prefabricated defects match section 2 (numerical simulation). Afterwards, the inspection system moves forward along the weld direction by a hand lever, then the system scans the prefabricated defects in succession. Furthermore, the vertical component samples of MFL signal for the rectangular slot defects in the weld and the rectangular slot defects in WHAZ under the different depths have been collected in the experiment. Then after the original signal samples are pretreated, it is shown in Figure 6 that the 3D distribution diagrams of MFL signal for the above two conditions are obtained.

The 2D curves for the optimal sampling point have been extracted respectively for each defect position from Figure 6, and these curves have been summarized in Figure 7. Then curves of MFL signal with the channel count change are obtained. In addition, from Figure 7, the peaks of LMF signal are

increasing with the defect depth increasing. Above conclusions are consistent with the numerical simulation.

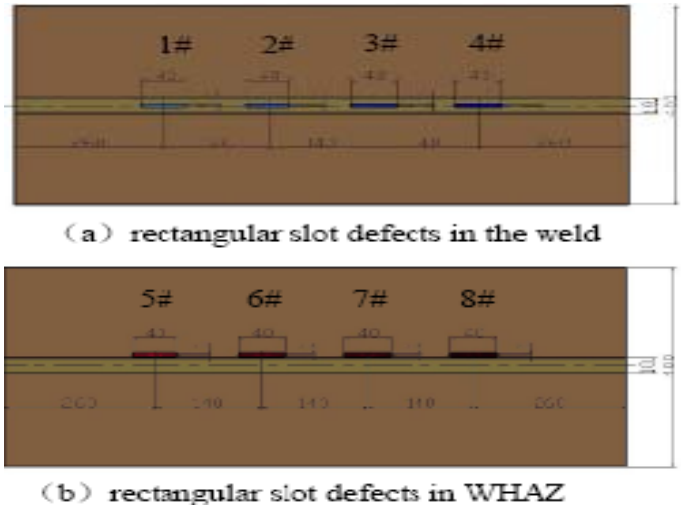


**Figure 5 : Diagram of the weld experiment board**

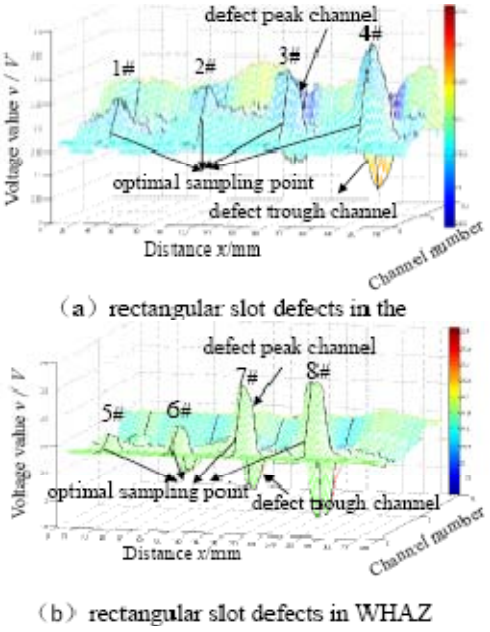


**Figure 6 : Diagram of MFL curves in the weld with different locations**

## Comparative analysis of the experimental and numerical study

Peaks of 1# ~4# defect of MFL signal of rectangular slot defects in the weld have been extracted from Figure 7(a), and then peaks of 5# ~8# defect of MFL signal of rectangular slot defects in WHAZ have been extracted from Figure 7(b). Also, extract with the corresponding numerical analysis in section 2, LMF peaks of $a_1$, $a_2$, $a_3$, $a_4$ defect of rectangular slot defects in the weld have been extracted from Figure 2(b), and LMF peaks of $b_1$, $b_2$, $b_3$, $b_4$ defect of rectangular slot defects in WHAZ have been extracted from Figure 3(b). Afterwards, Figure 8 shows the fitting curves by least squares method, and polynomial regression equation (2) - (5) for two kinds of positions are obtained. In addition, calculate correlation coefficient R between the simulation analysis original data and the experimental study data for each state of the weld, then rectangular slot defects in the weld $R_{wr}$ is 0.9764, and the similar degree between two results reaches 97.64%; rectangular slot defects in WHAZ $R_{hr}$ is 0.943, and the similar degree between two results reaches 94.3%.

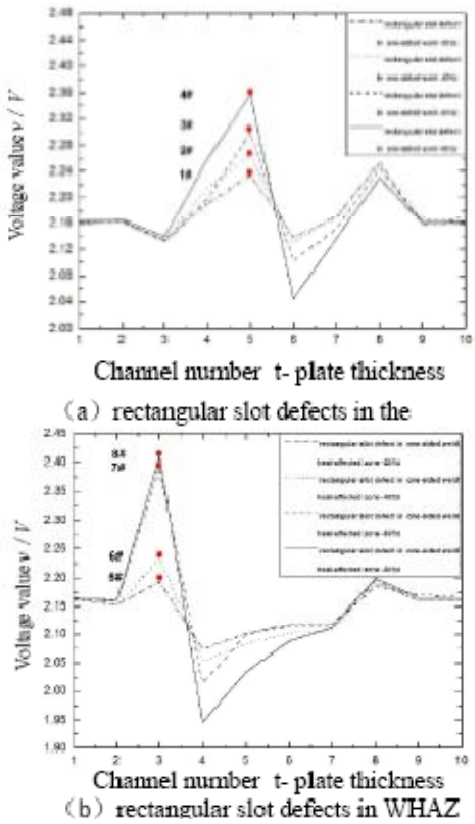


**Figure 7 : Contrast curves of MFL signal in the weld with different locations**

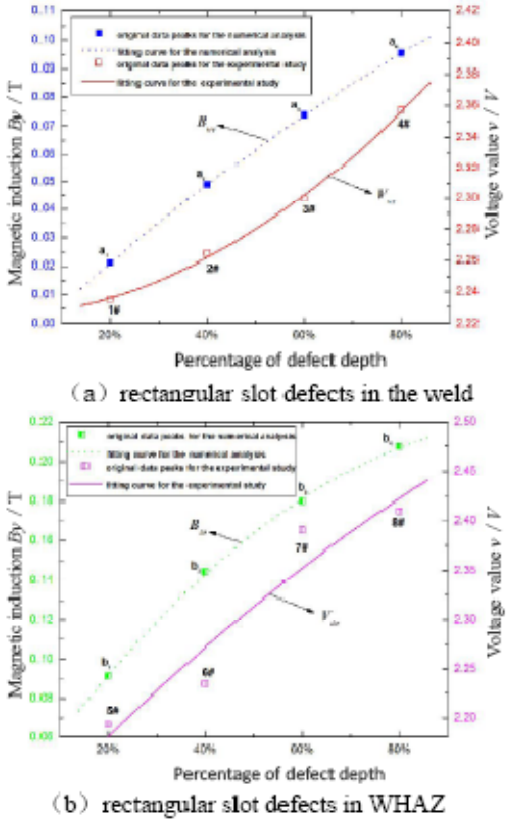


**Figure 8 : Fitting curves in the weld with different locations**

$$B_{wr} = -0.03971875 + 0.16357525 - 0.0101377 \quad (2)$$

Formula (2):
$B_{wr}$- LMF peaks of the rectangular slot defects in the weld for the numerical analysis (T);
*b*- percentage of defect depth.

$$V_{wr}=0.176875b^2+0.023875b+2.223975 \quad \textbf{(3)}$$

Formula (3):
$V_{wr}$- MFL signal peaks of the rectangular slot defects in the weld for the experimental study (V);
*b*- percentage of defect depth.

$$\mathbf{B_{hr}=-0.162525b^2+0.354361b+0.027261} \quad \textbf{(4)}$$

Formula (4):
$B_{hr}$- LMF peaks of the rectangular slot defects in WHAZ for the numerical analysis (T);
*b*- percentage of defect depth.

$$\mathbf{V_{hr}=-0.1325b^2+0.5357b+2.07885} \quad \textbf{(5)}$$

Formula (5):
$V_{hr}$- MFL signal peaks of the rectangular slot defects in WHAZ for the experimental study (V);
*b*- percentage of defect depth.

## CONCLUSION

Combining experimental method and FEM, and comparative analysis LMF samples in the weld with different locations, then verify the reliability and validity of the theory with experimental results, the following conclusions:

(1) 3D LMF models with rectangular slot in the weld with different locations have been established, also, numerical methods and simulation models of 3D LMF have been given.

(2) MFL signal curves by experimentally measuring consistent with the conclusions of the numerical analysis, and the correlation coefficient between the original data: the rectangular slot defects in the weld $R_{wr}$ **is** 0.9764; the rectangular slot defects in WHAZ $R_{hr}$ is 0.943. Furthermore, experimental results validate the accurate reliability of the numerical model in the weld LMF analysis, and it can reflect the distribution of the magnetic field intensity for the actual weld that the numerical simulation model is established in this research.

(3) According to the principle of least squares, the fitting curves and **polynomial regression equation for the** original data of the numerical analysis and the experimental study **in different positions of the weld** are obtained.

## ACKNOWLEDGEMENTS

This Research is funded by Northeast Petroleum University Youth Science Foundation (2013NQ133).

## REFERENCES

**[1]** Cui Wei, Dai Guang, Li Wei et al.; Imaging characteristics and Statistical Features Analysis of Magnetic Flux Leakage for the weld[J]. Pressure Vessel, **31(5)**, 58-64 **(2014)**.

**[2]** A.M.Chertov, A.C.Karloff, W.Perez et al.; In-process ultrasound NDE of resistance spot welds[J]. Insight - Non-Destructive Testing and Condition Monitoring, **54(5)**, 257-261 **(2012)**.

**[3]** D.Groslier, S.Pellerin, F.Valensi; Explorative approach of the spectral analysis tools to the detection of welding defects in lap welding[J]. Nondestructive Testing and Evaluation, **26(3)**, 13-18 **(2011)**.

**[4]** Du Dong, Cai Guo-rui, Tian Yuan et al.; Automatic Inspection of Weld Defects with X-Ray Real-Time Imaging[J]. Lecture Notes in Control and Information Sciences, **362**, 359-366 **(2007)**.
**[5]** Feng Xing-kui; Process equipment Welding [M]. Beijing: Chemical Industry Press, 60-62 **(2003)**.
**[6]** J.Mirapeix, P.B.Garcı´a-Allende, A.Cobo et al.; Real-time arc-welding defect detection and classification with principal component analysis and artificial neural networks[J]. NDT&E International, **40(2)**, 315-323 **(2007)**.
**[7]** Cui Wei, Dai Guang, Wang Xue-zeng; Study of One-sided Welding Surface Defects Based on the Method of Magnetic Flux Leakage[J]. Pressure Vessel, **30(2)**, 22-28 **(2013)**.